

DOI: 10.25702/KSC.2588-0039.2019.42.206-209

EMISSION INTENSITIES OF FIRST AND SECOND POSITIVE SYSTEM BANDS OF N₂ IN THE EARTH'S MIDDLE ATMOSPHERE DURING PRECIPITATIONS OF RELATIVISTIC ELECTRONS

A.S. Kirillov, V.B. Belakhovsky

Polar Geophysical Institute, Apatity, Murmansk region, Russia

Abstract. The main aim of the paper is the study of electronic kinetics of N₂ triplet states in the middle atmosphere during relativistic electrons penetrations taking into account collision processes at the altitudes. The results of calculations of emission intensities of first (749 nm and 669 nm) and second (337 nm) positive molecular nitrogen systems in the Earth's atmosphere during the precipitation of relativistic electrons (100 keV - 10 MeV) are presented. The calculation takes into account the quenching of triplet states of nitrogen in molecular collisions with the participation of N₂ and O₂ molecules. It is shown that there is a significant decrease in the emission rates of the bands of N₂ first positive system at lower altitudes in comparison with ones of the bands of N₂ second positive system.

1. Introduction

Relativistic electrons (with energy > 1 MeV) at near Earth space are produced at the outer radiation belt. The relativistic electron precipitation into the atmosphere is one of the main mechanisms of the losses of outer radiation belt. At altitude about 50 km the relativistic electron precipitations excite bremsstrahlung which can reach the altitude 20 km. At these altitudes bremsstrahlung is detected by X-ray detectors on the stratospheric balloons [Millan *et al.*, 2002].

The interaction of energetic electrons with main atmospheric components N₂ and O₂ is an important mechanism of ionization and dissociation in the middle atmosphere causing the production of odd nitrogen (NO_x) and odd-hydrogen (HO_x) [Turunen *et al.*, 2009; Newnham *et al.*, 2018]. Enhanced concentrations of these minor atmospheric components during relativistic electron precipitations lead to catalytic ozone loss [Roldugin *et al.*, 2000; Seppälä *et al.*, 2015; Turunen *et al.*, 2016] changing atmospheric heating and cooling balance.

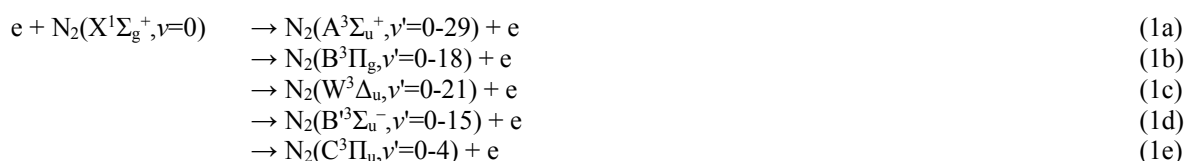
Also, energetic relativistic electrons penetrating in the upper and middle atmosphere lead to electronic and vibrational excitation of main atmospheric components. Artamonov *et al.* [2016, 2017] have presented profiles of enhanced ionization rates in the upper and middle atmosphere induced by relativistic electrons with energies 100 keV-100 MeV. One of the indicators of the state of the Earth's atmosphere is optical emissions of atmospheric components. Since N₂ gas dominates in the composition of the Earth's atmosphere, the atmospheric emission spectra have to contain a manifold of molecular nitrogen bands radiated from electronically excited states.

Main aim of the paper is the study of electronic kinetics of N₂ triplet states in the middle atmosphere during relativistic electron precipitations taking into account collision processes at these altitudes. We will consider the influence of the inelastic molecular collisions on volume and column intensities of N₂ first and second positive bands.

2. The model of N₂ electronic kinetics in the middle atmosphere

We apply here the model of N₂ electronic kinetics in the middle atmosphere presented by Kirillov and Belakhovsky [2019]. The authors have taken into account all intramolecular and intermolecular electron energy transfers in the electronic quenching of electronically excited triplet nitrogen N₂(A³Σ_u⁺, B³Π_g, W³Δ_u, B³Σ_u⁻, C³Π_u) by the collisions with N₂ and O₂ molecules considered by Kirillov [2010, 2011, 2016, 2019]. It was shown by Kirillov and Belakhovsky [2019] that both intramolecular and intermolecular transfer processes are very important in the calculation of vibrational populations of N₂ triplet states at the altitudes of the middle atmosphere.

The model includes the consideration of the excitation of five electronic states of molecular nitrogen in the collisions of N₂(X¹Σ_g⁺, v=0) by high-energetic electrons in the middle atmosphere of the Earth



The rates of the excitation of vibrational levels of all five states are proportional to the Franck-Condon factor $q_{0v'}^{xy}$ of the transition $X^1\Sigma_g^+, v=0 \rightarrow Y, v'$ where $Y=A^3\Sigma_u^+, B^3\Pi_g, W^3\Delta_u, B^3\Sigma_u^-, C^3\Pi_u$ [Gilmore *et al.*, 1992].

The electronically excited molecules radiate the bands of Vegard-Kaplan (VK), First Positive (1PG), Wu-Benesch (WB), Afterglow (AG), Second Positive (2PG) systems:



Einstein coefficients for the radiational transitions (2a-2e) are taken according to [Gilmore *et al.*, 1992] in our calculations.

To calculate vibrational populations N of the $\text{A}^3\Sigma_u^+$, $\text{B}^3\Pi_g$, $\text{W}^3\Delta_u$, $\text{B}^1\Sigma_u^-$, $\text{C}^3\Pi_u$ triplet states we apply the following equations by Kirillov and Belakhovsky [2019]

$$\begin{aligned} & Q^Y q_{0\nu'}^{XY} + \sum_{\nu''} A_{\nu''\nu'}^{BY} N_{\nu''}^B + \sum_{\nu''} k_{\nu''\nu'}^{*BY} N_{\nu''}^B ([N_2] + [O_2]) + \sum_{Z, \nu''} k_{\nu''\nu'}^{**ZY} N_{\nu''}^Z [N_2] + \\ & + \sum_{\nu''} k_{\nu''\nu'}^{**BY} N_{\nu''}^B [N_2] + \sum_{\nu''} k_{\nu''\nu'}^{**CY} N_{\nu''}^C [N_2] = \\ & = \left\{ \sum_{\nu''} A_{\nu''\nu'}^{YB} + A_{\nu''\nu'}^Y + \sum_{\nu''} k_{\nu''\nu'}^{*YB} ([N_2] + [O_2]) + \sum_{Z, \nu''} k_{\nu''\nu'}^{**YZ} [N_2] + \sum_{\nu''} k_{\nu''\nu'}^{**YB} [N_2] + k_{\nu''\nu'}^{**Y} [O_2] \right\} N_{\nu'}^Y \end{aligned} \quad (3a)$$

$$\begin{aligned} & Q^B q_{0\nu'}^{XB} + \sum_{Y, \nu''} A_{\nu''\nu'}^{YB} N_{\nu''}^Y + \sum_{\nu''} A_{\nu''\nu'}^{CB} N_{\nu''}^C + \sum_{Y, \nu''} k_{\nu''\nu'}^{*YB} N_{\nu''}^Y ([N_2] + [O_2]) + \\ & + \sum_{Y, \nu''} k_{\nu''\nu'}^{**YB} N_{\nu''}^Y [N_2] + \sum_{\nu''} k_{\nu''\nu'}^{**BB} N_{\nu''}^B [N_2] + \sum_{\nu''} k_{\nu''\nu'}^{**CB} N_{\nu''}^C [N_2] = \\ & = \left\{ \sum_{Y, \nu''} A_{\nu''\nu'}^{BY} + \sum_{Y, \nu''} k_{\nu''\nu'}^{*BY} ([N_2] + [O_2]) + \sum_{Y, \nu''} k_{\nu''\nu'}^{**BY} [N_2] + \sum_{\nu''} k_{\nu''\nu'}^{**BB} [N_2] + k_{\nu''\nu'}^{**B} [O_2] \right\} N_{\nu'}^B \end{aligned} \quad (3b)$$

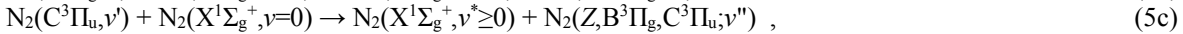
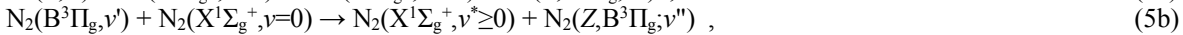
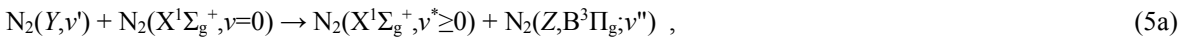
$$\begin{aligned} & Q^C q_{0\nu'}^{XC} + \sum_{\nu'' > \nu'} k_{\nu''\nu'}^{**CC} N_{\nu''}^C [N_2] = \\ & = \left\{ \sum_{\nu''} A_{\nu''\nu'}^{CB} + \sum_{Y, \nu''} k_{\nu''\nu'}^{**CY} [N_2] + \sum_{\nu''} k_{\nu''\nu'}^{**CB} [N_2] + \sum_{\nu'' < \nu'} k_{\nu''\nu'}^{**CC} [N_2] + k_{\nu''\nu'}^{**C} [O_2] \right\} N_{\nu'}^C \end{aligned} \quad (3c)$$

where Y and $Z = \text{A}^3\Sigma_u^+$, $\text{W}^3\Delta_u$, $\text{B}^1\Sigma_u^-$; Q^Y , Q^B , Q^C are production rates of the Y -th, $\text{B}^3\Pi_g$, $\text{C}^3\Pi_u$ states, respectively; A are spontaneous radiational probabilities for the transitions (2b-2e); k^* and k^{**} mean the constants of intramolecular and intermolecular electron energy transfer processes, respectively; $A_{\nu''\nu'}^Y$ means radiational probability of the transition (2a) for the $\text{A}^3\Sigma_u^+$ state and $A_{\nu''\nu'}^Y = 0$ for the $\text{W}^3\Delta_u$ and $\text{B}^1\Sigma_u^-$ states.

Here we consider the following intramolecular processes:

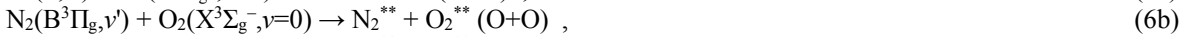


with $Y = \text{A}^3\Sigma_u^+$, $\text{W}^3\Delta_u$, $\text{B}^1\Sigma_u^-$,
intermolecular processes:



with Y and $Z = \text{A}^3\Sigma_u^+$, $\text{W}^3\Delta_u$, $\text{B}^1\Sigma_u^-$ for the inelastic collisions with N_2 molecules,

and the electronic quenching by O_2 with the transfer of the excitation energy on the oxygen molecules:



where $Y = \text{A}^3\Sigma_u^+$, $\text{W}^3\Delta_u$, $\text{B}^1\Sigma_u^-$ and N_2^{**} , O_2^{**} means electronically or vibrationally excited molecules and the energy transfer processes (6a-6c) can cause the excitation of repulsive states of O_2 with the dissociation of oxygen molecules

[Kirillov, 2011]. The rates of the processes (4a,4b), (5a-5c) and (6a-6c) are presented by Kirillov and Belakhovsky [2019].

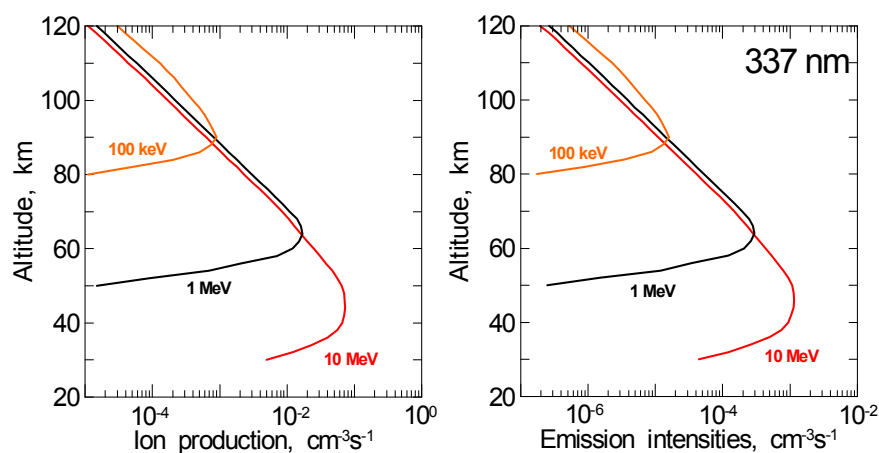


Figure 1. The altitude profiles of ionization rates by Artamonov *et al.* [2017] and calculated volume intensities of 337 nm N₂ emission for three energies of relativistic electrons 100 keV, 1 MeV, 10 MeV.

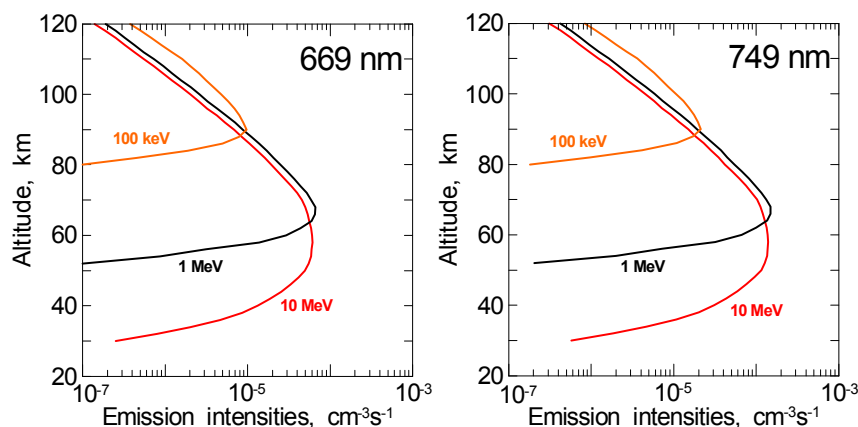


Figure 2. The altitude profiles of calculated volume intensities of 669 and 749 nm N₂ emissions for three energies of relativistic electrons 100 keV, 1 MeV, 10 MeV.

3. The calculation of intensity profiles for N₂ first and second positive bands

The altitude profiles of calculated ionization rates in the middle atmosphere during relativistic electrons penetrations have been presented by Artamonov *et al.* [2017]. Authors have calculated the ion productions for isotropic monoenergetic electrons in the energy range 100 keV–100 MeV suggesting $\epsilon=35$ eV as the average energy necessary for production of an ion pair in air. The calculation has shown that ionization rates in the isotropic case have two peaks. The first peak is related to the direct ionization of ambient air, the second is due to bremsstrahlung.

We consider here only the rates related to the direct ionization of ambient air for relativistic electrons penetrations with energies of 100 keV – 10 MeV. The method of degradation spectra [Konovalov, 1993] was applied in the calculation of average energies ϵ necessary for the excitation of N₂ triplet states by energetic secondary electrons in the processes (1a-1e).

The altitude profiles of ion production according to the calculations by Artamonov *et al.* [2017] for three energies of relativistic electrons 100 keV, 1 MeV and 10 MeV are shown in Fig. 1. Here we consider the profiles of ionization rates without ionization induced by bremsstrahlung. Also, the calculated volume intensities of 337 nm N₂ emission are presented in Fig. 1 at the same energies of electrons. The radiation of N₂ second positive 337 nm emission is related with the transitions (2e) $v'=0 \rightarrow v''=0$. Fig. 1 shows that the altitude profiles of volume intensities of the 337 nm N₂ emission correlate with the profiles of ion production by Artamonov *et al.* [2017].

Also, the calculated volume intensities of 669 nm and 749 nm N₂ first positive emissions are presented in Fig. 2. The radiation of N₂ first positive 669 nm and 749 nm emissions is related with the transitions (2b) $v'=5 \rightarrow v''=2$ and $v'=4 \rightarrow v''=2$, respectively. The altitude profiles of volume intensities of 669 nm and 749 nm emissions show significant decrease in comparison with the intensity of 337 nm emission at the altitudes below ~60 km. The decrease can be explained by effective quenching of the B³Π_g state in molecular processes (4b), (5b), (6b).

The dependence of the calculated column intensity ratios $I(749\text{ nm})/I(337\text{ nm})$ and $I(669\text{ nm})/I(337\text{ nm})$ on energies of relativistic electrons is presented in Table 1. Also, we show here the same ratios calculated using auroral rocket observations on Hays Island on 13.12.1972 published by Kirillov *et al.* [1987]. There is an agreement of the calculated column intensity ratios at the relativistic electron energy of 100 keV with the results of auroral rocket observations. The intensity ratios of first and second positive bands depend on the energy of precipitating relativistic electrons and could be applied as an indicator of mean energy of the high-energetic particles.

Table 1. The calculated column intensity ratios $I(749\text{ nm})/I(337\text{ nm})$ and $I(669\text{ nm})/I(337\text{ nm})$ on energies of relativistic electrons $E=100\text{ keV} - 10\text{ MeV}$.

	<i>Kirillov et al.</i> [1987]	100 keV	500 keV	1 MeV	5 MeV	10 MeV
$I(749\text{ nm})/I(337\text{ nm})$	1.58 ($\pm 30\%$)	1.41	0.92	0.61	0.25	0.17
$I(669\text{ nm})/I(337\text{ nm})$	0.65 ($\pm 30\%$)	0.64	0.42	0.27	0.11	0.074

4. Conclusions

The altitude profiles of the calculated volume intensities of 337 nm, 669 nm, 749 nm N₂ emissions in the middle atmosphere are presented for the cases of relativistic electrons penetrations. The calculations are made for energies of relativistic electrons [Artamonov *et al.*, 2017] 100 keV – 10 MeV. The electronic kinetics of N₂ triplet states $A^3\Sigma_u^+$, $B^3\Pi_g$, $W^3\Delta_u$, $B^3\Sigma_u^-$, $C^3\Pi_u$ in the middle atmosphere of the Earth during relativistic electron precipitation is considered. Intramolecular and intermolecular electron energy transfers in inelastic collisions of electronically excited molecular nitrogen with N₂ and O₂ molecules are taken into account in the calculations.

It is shown that there is a dependence of the calculated column intensity ratios of first and second positive bands on the energy of relativistic electrons. The calculated column intensity ratios $I(749\text{ nm})/I(337\text{ nm})$ and $I(669\text{ nm})/I(337\text{ nm})$ decrease with increasing relativistic electron energy. This fact can be explained by more effective contribution of the quenching processes in vibrational populations of the $B^3\Pi_g$ state than of the $C^3\Pi_u$ state at lower altitudes.

Acknowledgements. This work is supported by the Russian Science Foundation (Project # 18-77-10018).

References

- Artamonov A.A., Mishev A.L., Usoskin I.G. Model CRAC: EPII for atmospheric ionization due to precipitating electrons: Yield functions and applications. 2016, *J. Geophys. Res.: Space Phys.*, v.121, p.1736-1743.
- Artamonov A., Mironova I., Kovaltsov G. et al. Calculation of atmospheric ionization induced by electrons with non-vertical precipitation: Updated model CRAC-EPII. 2017, *Adv. Space Res.*, v.59, p.2295-2300.
- Gilmore F.R., Laher R.R., Espy P.J. Franck-Condon factors, r-centroids, electronic transition moments, and Einstein coefficients for many nitrogen and oxygen band systems. 1992, *J. Phys. Chem. Ref. Data*, v.21, p.1005-1107.
- Kirillov A.S. Electronic kinetics of molecular nitrogen and molecular oxygen in high-latitude lower thermosphere and mesosphere. 2010, *Ann. Geophys.*, v.28, p.181-192.
- Kirillov A.S. Excitation and quenching of ultraviolet nitrogen bands in the mixture of N₂ and O₂ molecules. 2011, *J. Quan. Spec. Rad. Tran.*, v.112, p.2164-2174.
- Kirillov A.S. Intermolecular electron energy transfer processes in the collisions of N₂($A^3\Sigma_u^+$, $\nu=0-10$) with CO and N₂ molecules. 2016, *Chem. Phys. Lett.*, v.643, p.131-136.
- Kirillov A.S. Intermolecular electron energy transfer processes in the quenching of N₂($C^3\Pi_u$, $\nu=0-4$) by collisions with N₂ molecules. 2019, *Chem. Phys. Lett.*, v.715, p.263-267.
- Kirillov A.S., Belakhovsky V.B. The kinetics of N₂ triplet electronic states in the upper and middle atmosphere during relativistic electron precipitation. 2019, *Geophys. Res. Lett.*, v.46, p.7734-7743.
- Kirillov A.S., Yagodkina O.I., Ivanov V.E., Vorobjev V.G. Excitation mechanisms of IPG N₂ system in aurora. 1987, *Geomag. Aeron.*, v.27, p.419-427.
- Konovalov V.P. Degradation electron spectrum in nitrogen, oxygen and air. 1993, *Tech. Phys.*, v.63(3), p.23-33.
- Millan R.M., Lin R.P., Smith D.M. et al. X-ray observations of MeV electron precipitation with a balloon-borne germanium spectrometer. 2002, *Geophys. Res. Lett.*, v.29(24), 2194.
- Newnham D.A., Clilverd M.A., Rodger C.J. et al. Observations and modeling of increased nitric oxide in the Antarctic polar middle atmosphere associated with geomagnetic storm-driven energetic electron precipitation. 2018, *J. Geophys. Res.: Space Phys.*, v.123, p.6009-6025.
- Roldugin V.C., Beloglazov M.I., Remenets G.F. Total ozone decrease in the Arctic after REP events. 2000, *Ann. Geophys.*, v.18, p.332-336.
- Seppälä A., Clilverd M.A., Beharrell M.J. et al. Substorm-induced energetic electron precipitation: Impact on atmospheric chemistry. 2015, *Geophys. Res. Lett.*, v.42, p.8172-8176.
- Turunen E., Verronen P.T. et al. Impact of different energies of precipitating particles on NO_x generation in the middle and upper atmosphere during geomagnetic storms. 2009, *J. Atmos. Sol. Terr. Phys.*, v.71, p.1176-1189.
- Turunen E., Kero A., Verronen P.T. et al. Mesospheric ozone destruction by high-energy electron precipitation associated with pulsating aurora. 2016, *J. Geophys. Res.: Atmos.*, v.121, p.11852-11861.